

## **Facet-engineering of NH<sub>2</sub>-UiO-66 with Enhanced Photocatalytic Hydrogen Production Performance**

Xiaofan Shi,<sup>a</sup> Xin Lian,<sup>a</sup> Di Yang,<sup>a</sup> Xiaojuan Hu,<sup>c</sup> Jijie Zhang\*<sup>a</sup> and Xian-He Bu<sup>a,b</sup>

*<sup>a</sup>School of Materials Science and Engineering, Tianjin Key Laboratory of Metal and Molecule-Based Material Chemistry, Nankai University, Tianjin 300350, China.*

*<sup>b</sup>State Key Laboratory of Elemento-Organic Chemistry, College of Chemistry, Nankai University, Tianjin 300071, China.*

*<sup>c</sup>Fritz-Haber-Institut der Max-Planck-Gesellschaft, Faradayweg 4-6, Berlin 14195, Germany.*

Corresponding author: zhangjijie@nankai.edu.cn

**Table S1.** Reactants' concentration and reaction time of different NH<sub>2</sub>-UiO-66 samples.

<b>Morphology</b>	<b>c(ZrCl<sub>4</sub>) (mmol/L)</b>	<b>c(NH<sub>2</sub>-BDC) (mmol/L)</b>	<b>Equivalent of HF acid</b>	<b>Reaction time (h)</b>
<b>Cube</b>	3	3	2	24
<b>Tetra- decahedron</b>	6	6	4	12
<b>Octahedron</b>	36	36	4	12

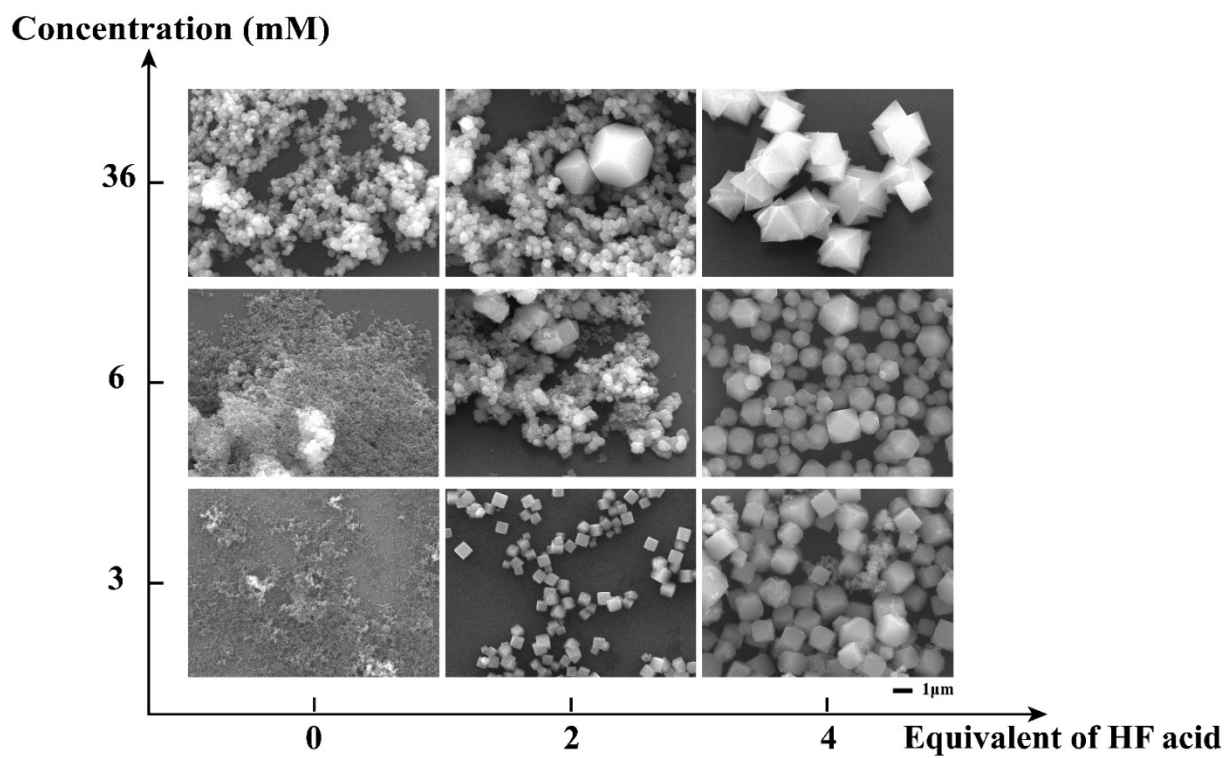


**Figure S1.** Morphology of  $\text{NH}_2\text{-UiO-66}$  in different reactants' concentration and specific equivalent of hydrofluoric acid.

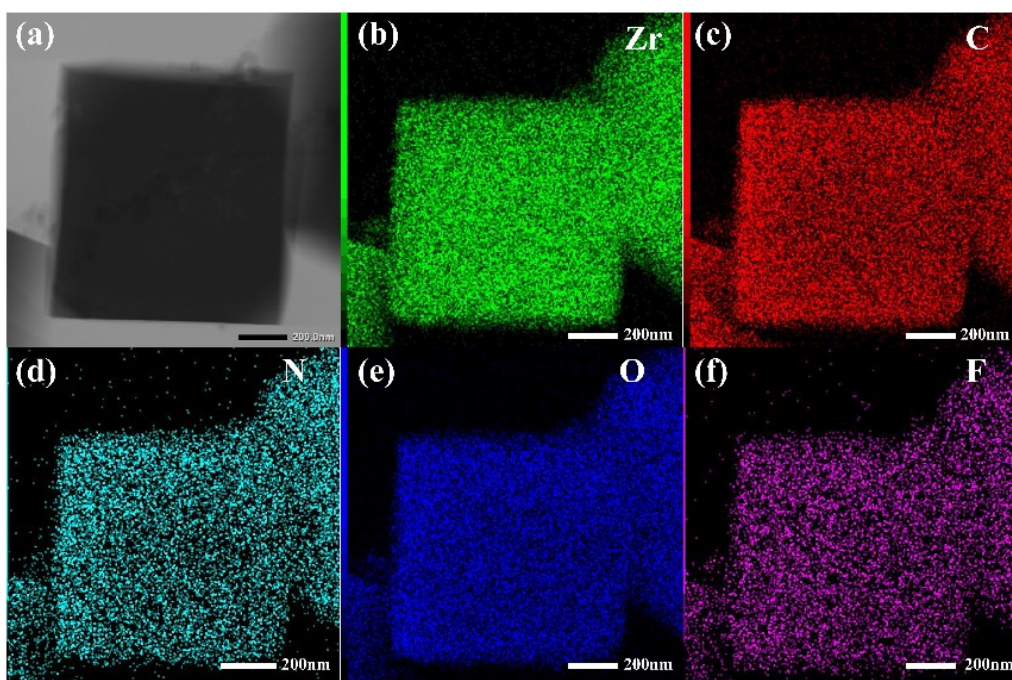


**Figure S2.** (a) TEM and (b-f) mapping images of C-UiO.

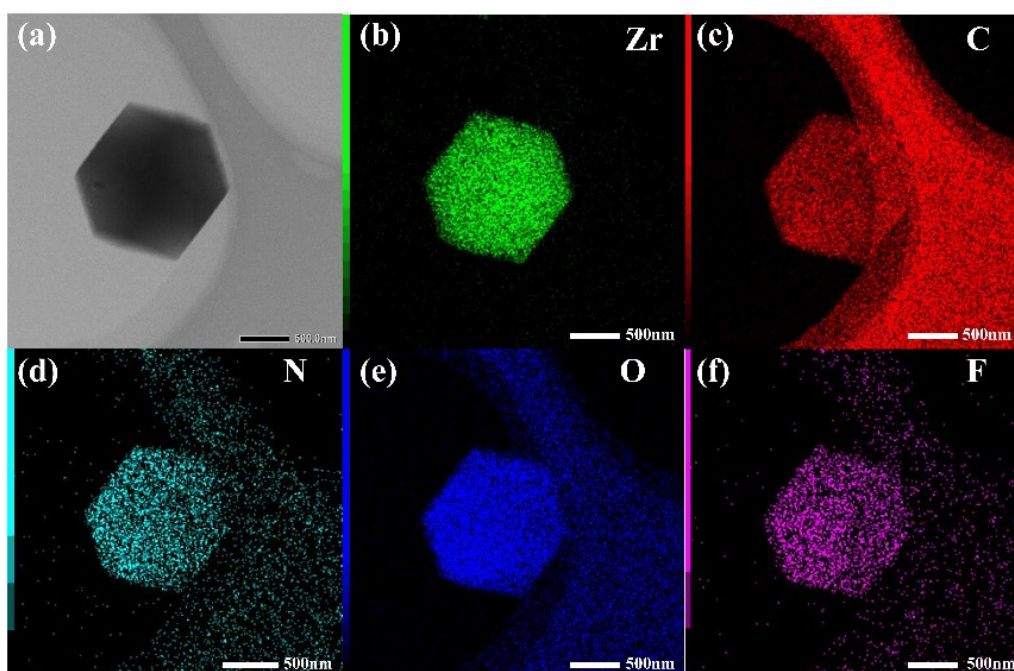


**Figure S3.** (a) TEM and (b-f) mapping images of T-UiO.

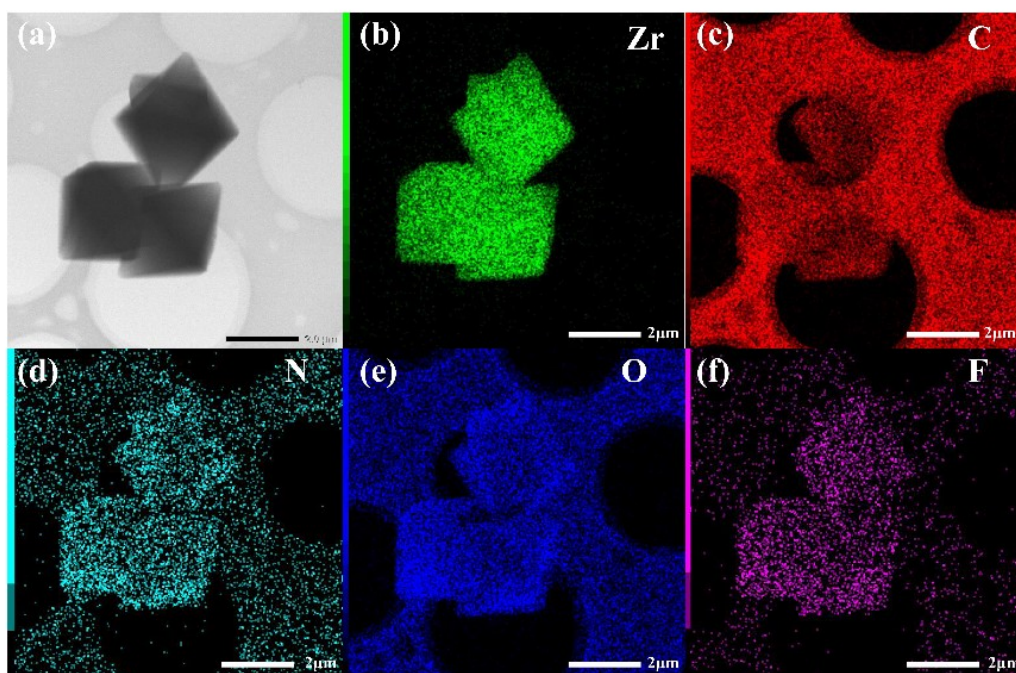


**Figure S4.** (a) TEM and (b-f) mapping images of O-UiO.

**Table S2.** Specific binding energy location of samples.

Samples	Zr3d <sub>3/2</sub>	Zr3d <sub>5/2</sub>
<b>C-UiO</b>	185.58 eV	183.21 eV
<b>T-UiO</b>	185.53 eV	183.16 eV
<b>O-UiO</b>	185.62 eV	183.25 eV
<b>NH<sub>2</sub>-UiO-66 with HAc</b>	185.38 eV	183.02 eV

**Table S3.** Atomic concentration (%) of C1s, N1s, O1s, F1s, and Zr3d in C-UiO, T-UiO, and O-UiO determined by XPS.

	C	N	O	F	Zr
<b>C-UiO</b>	54.60	5.04	28.18	5.11	7.07
<b>T-UiO</b>	58.39	4.80	25.43	4.84	6.54
<b>O-UiO</b>	54.52	5.48	27.81	5.28	6.91

**Table S4.** Parameters of equivalent circuit for the impedance data of C-UiO, T-UiO and O-UiO.

Samples	$R_s(\Omega)$	$R_t(k\Omega)$
<b>C-UiO</b>	30.23	$3.50 \times 10^3$
<b>T-UiO</b>	29.26	$1.24 \times 10^3$
<b>O-UiO</b>	31.86	$2.67 \times 10^3$

**Table S5.** Fitting results of the time-resolved PL spectra of C-UiO, T-UiO and O-UiO.

Samples	$A_1(\%)$	$\tau_1(ns)$	$A_2(\%)$	$\tau_2(ns)$	$\tau_{ave}(ns)$
<b>C-UiO</b>	0.79	0.71	0.21	4.71	3.15
<b>T-UiO</b>	0.79	0.59	0.21	6.71	5.20
<b>O-UiO</b>	0.87	0.56	0.13	6.05	3.99

**Table S6.** Fitting results of the TA kinetics of C-UiO, T-UiO and O-UiO.

Samples	$A_1(\%)$	$\tau_1(ps)$	$A_2(\%)$	$\tau_2(ps)$	$\tau_{ave}(ps)$
<b>C-UiO</b>	42.4	$78 \pm 8$	57.6	$1406 \pm 137$	$1341 \pm 255$
<b>T-UiO</b>	48.0	$23 \pm 4$	52.0	$610 \pm 26$	$590 \pm 29$
<b>O-UiO</b>	49.2	$19 \pm 4$	50.8	$875 \pm 76$	$858 \pm 80$

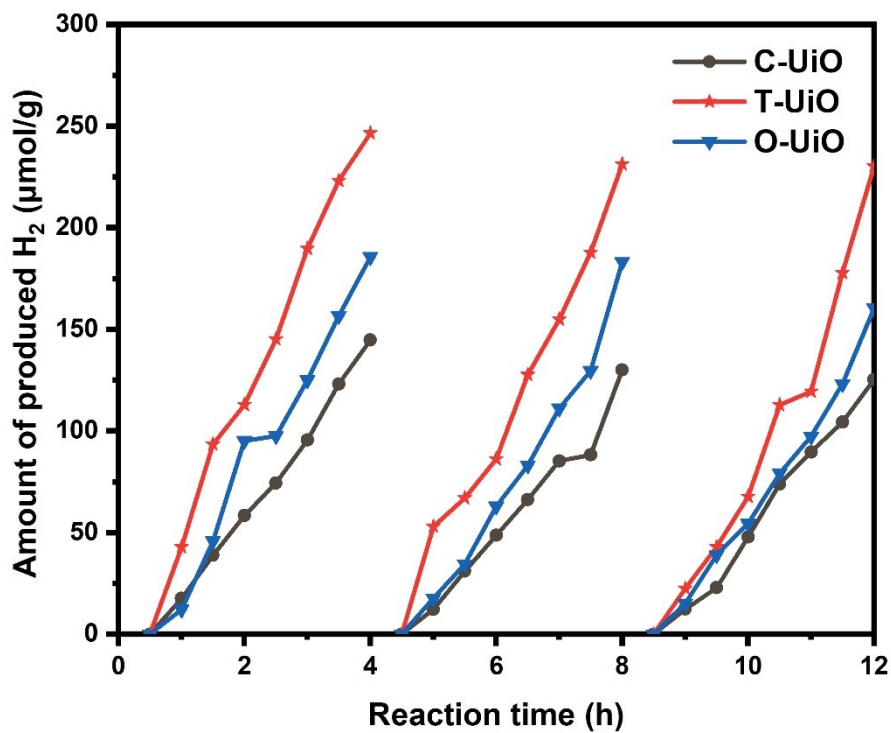


Figure S5. Photocatalytic recycling tests of different  $\text{NH}_2\text{-UiO-66}$  samples.

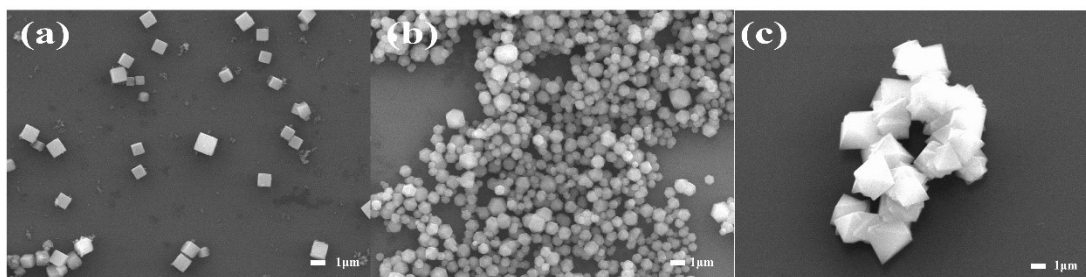
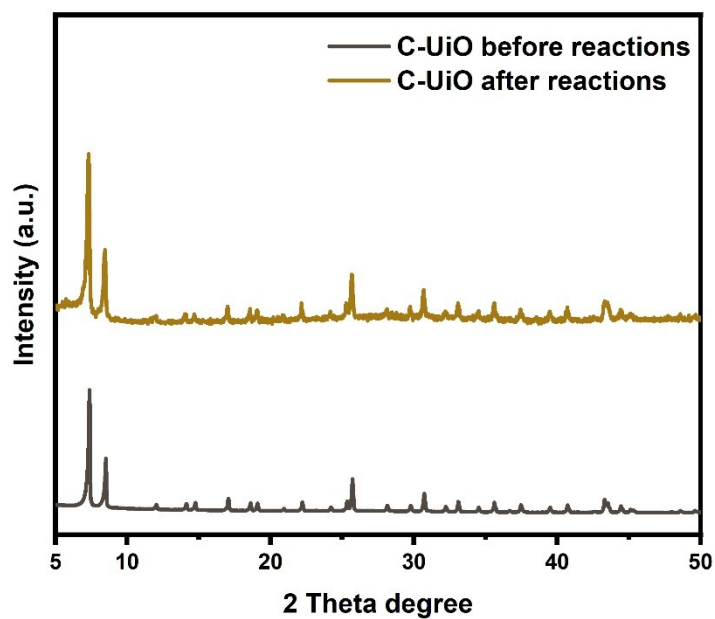
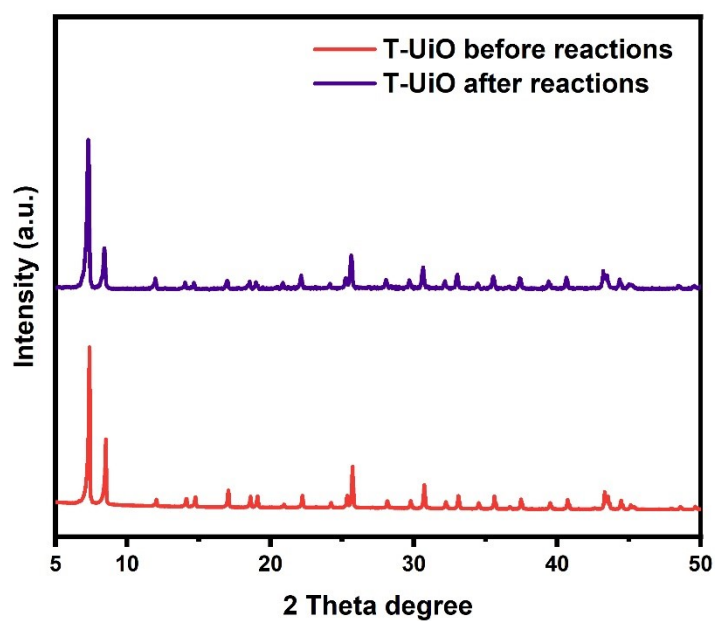


Figure S6. SEM images of (a) C-UiO, (b) T-UiO, (c) O-UiO samples after photocatalytic hydrogen reactions.



**Figure S7.** XRD patterns of C-UiO samples before and after photocatalytic hydrogen reactions.



**Figure S8.** XRD patterns of T-UiO samples before and after photocatalytic hydrogen reactions.

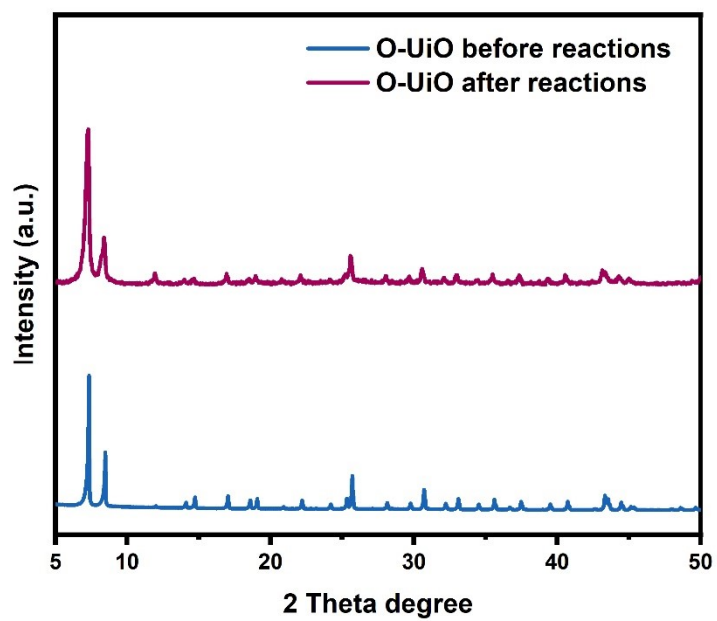


**Figure S9.** XRD patterns of O-UiO samples before and after photocatalytic hydrogen reactions.

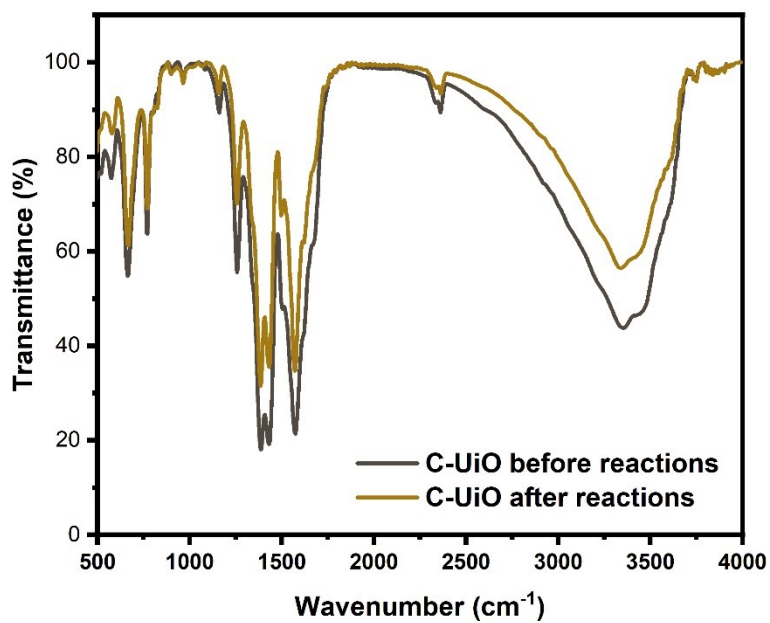


**Figure S10.** FT-IR spectra of C-UiO samples before and after photocatalytic hydrogen reactions.

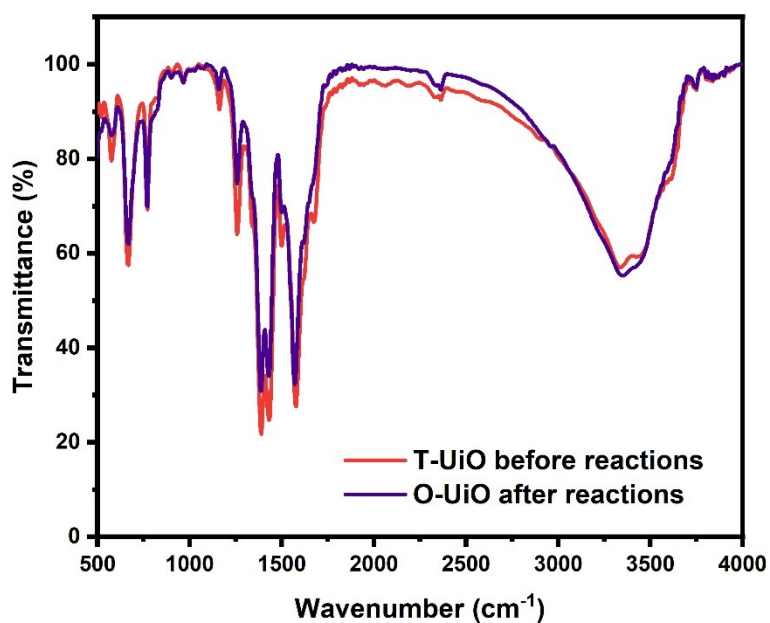


**Figure S11.** FT-IR spectra of T-UiO samples before and after photocatalytic hydrogen reactions.

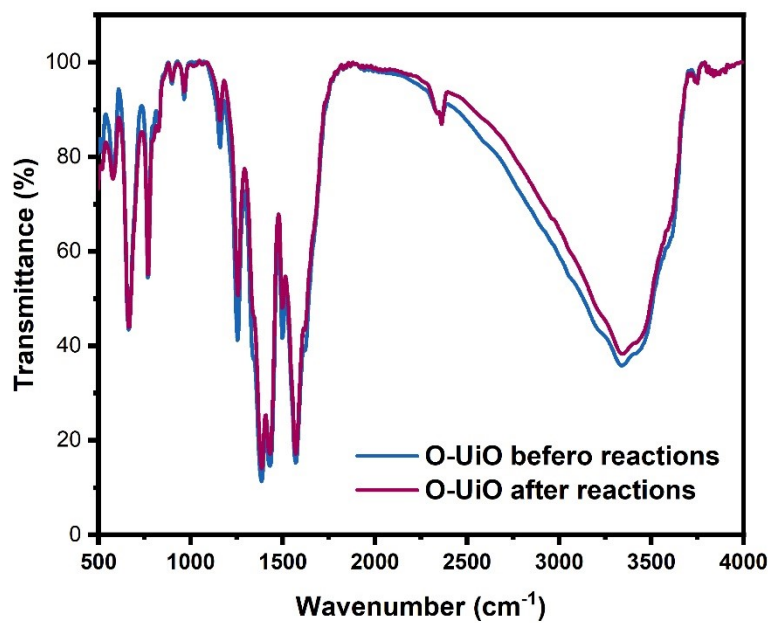


**Figure S12.** FT-IR spectra of O-UiO samples before and after photocatalytic hydrogen reactions.

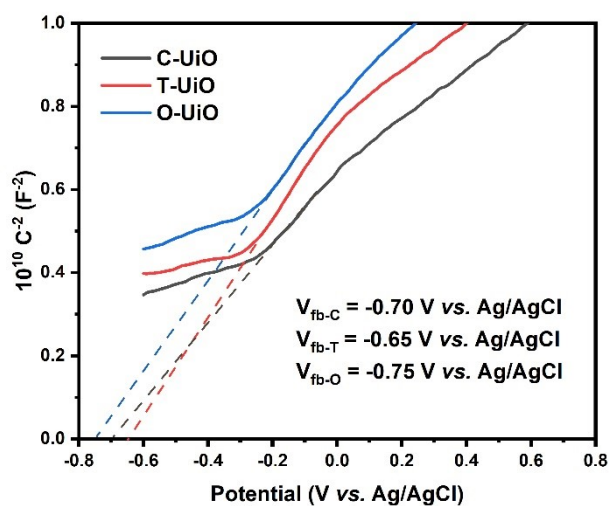


**Figure S13.** Mott-Schottky plots of different NH<sub>2</sub>-UiO-66 samples.

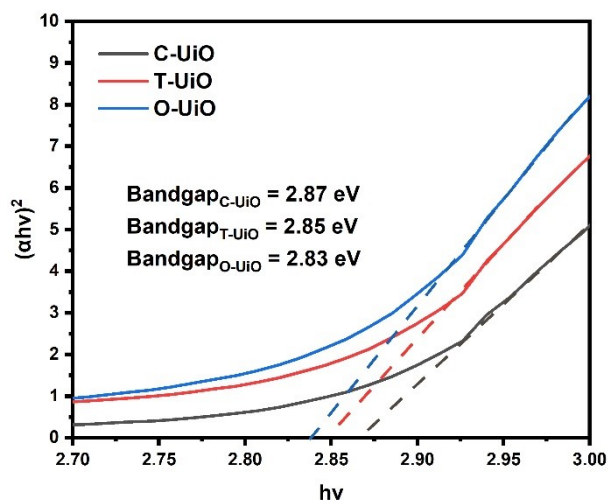


**Figure S14.** Tauc-plots of different NH<sub>2</sub>-UiO-66 samples.

**Table S7.** Band structure data of C-UiO, T-UiO, and O-UiO.

Samples	HOMO (eV)	LUMO (eV)	Band gap (eV)
<b>C-UiO</b>	2.77	-0.10	2.87
<b>T-UiO</b>	2.80	-0.05	2.85
<b>O-UiO</b>	2.68	-0.15	2.83

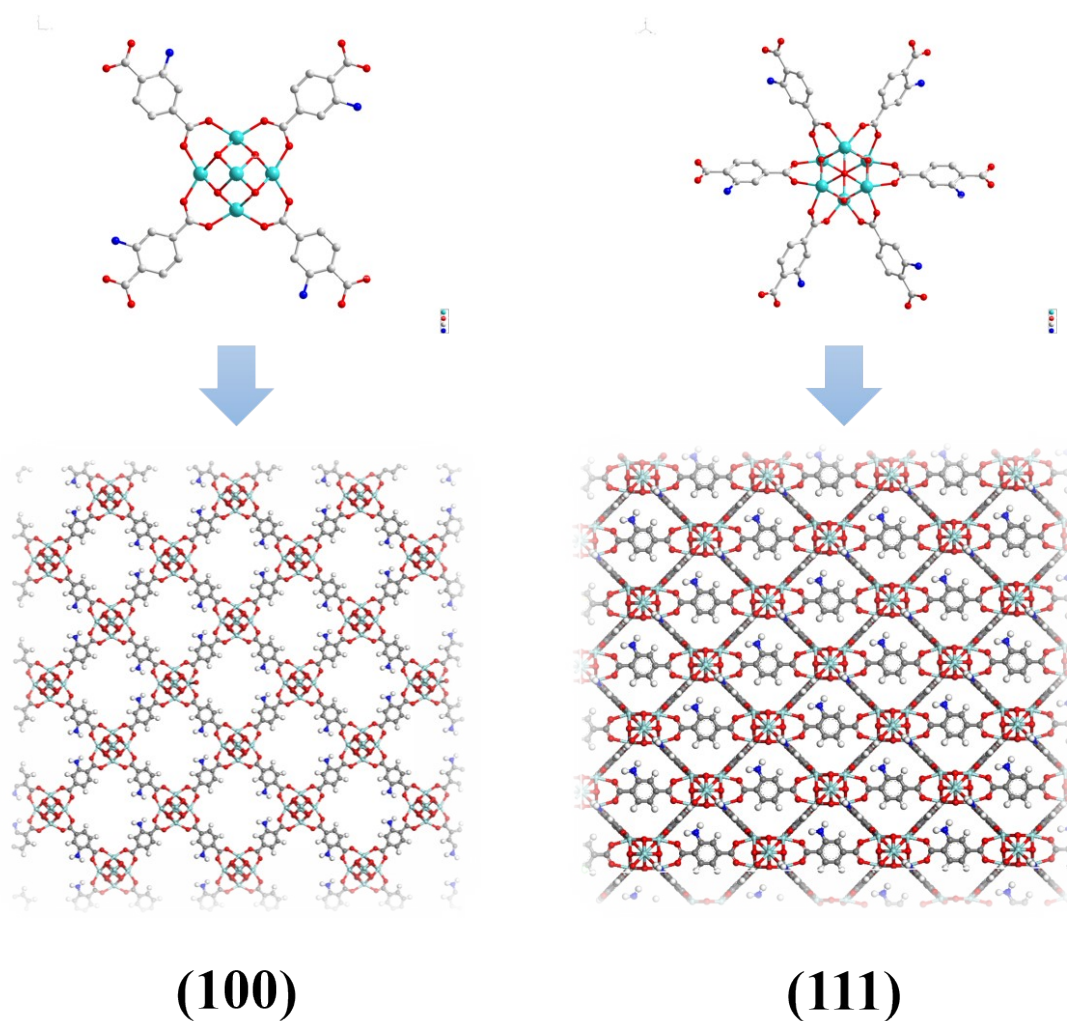


**Figure S15.** Coordination mode and structure of (100) and (111) facets.

To study the surface energy and DOS of these models, first-principles calculations were carried out using density functional theory (DFT) with generalized gradient approximation (GGA) of Perdew-Burke-Ernzerhof (PBE) implemented in the Vienna Ab-Initio Simulation Package (VASP).<sup>1, 2</sup> The valence electronic states were expanded based on plane waves with the core-valence interaction represented using the projector augmented plane wave (PAW) approach and a cutoff of 450 eV.<sup>3</sup> All atoms in the models were relaxed until the residual force was less than 0.05eV/Å.

The original bulk structure of NH<sub>2</sub>-UiO-66 was obtained from the Cambridge Crystallographic Data Centre (CCDC). The surface model of (100) and (111) facets

were cleaved from the optimized bulk NH<sub>2</sub>-UiO-66 model with a vacuum thickness of 25 Å to suppress the interaction between adjacent slabs. The Brillouin zone integration was sampled with 1x1x1 K-point meshes for geometry optimization. The surface energy of each facet ( $\gamma_{hkl}$ ) was calculated by the following formula:<sup>4</sup>

$$\gamma_{hkl} = \frac{E_{slab} - E_{bulk} - nE_{mol}}{A}$$

The  $E_{slab}$  is the total energy of the relaxed surface model. The  $E_{bulk}$  is the total energy of atoms that corresponding to the slab model in the original bulk system. The  $E_{mol}$  is the energy of small molecules we insert to maintain the chemometric ratio.  $A$  is the surface area of cleaved slab.

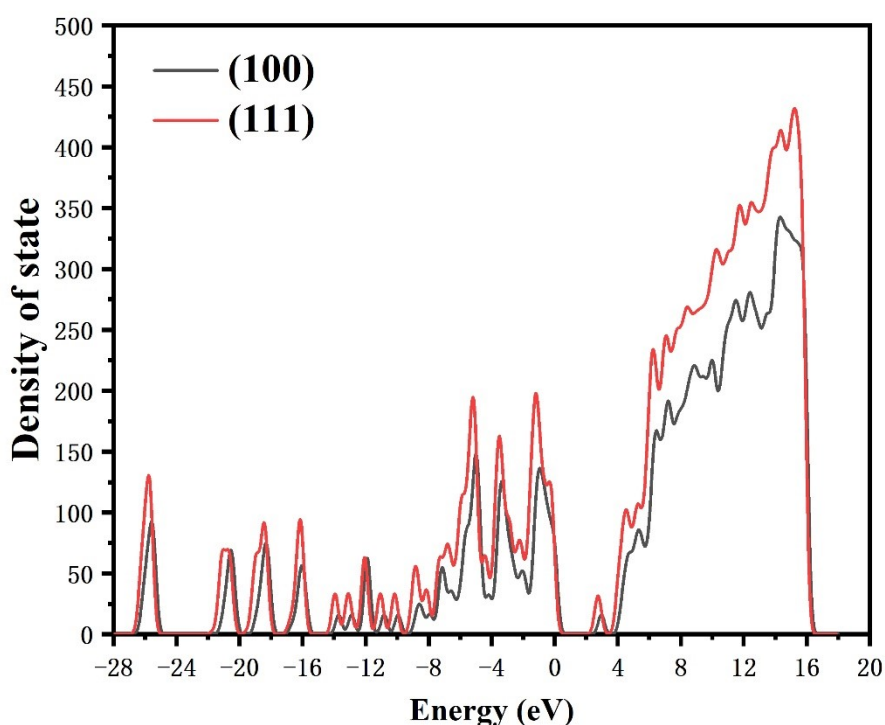


**Figure S16.** Density of states of (100) and (111) facets.

## REFERENCE

1. J. P. Perdew, K. Burke and M. Ernzerhof, *Phys. Rev. Lett.*, 1996, **77**, 3865-3868.
2. Kresse and Furthmuller, *Phys. Rev. B: Condens. Matter*, 1996, **54**, 11169-11186.
3. Blochl, *Phys. Rev. B: Condens. Matter*, 1994, **50**, 17953-17979.
4. F. Guo, J.-H. Guo, P. Wang, Y.-S. Kang, Y. Liu, J. Zhao and W.-Y. Sun, *Chem. Sci.*, 2019, **10**, 4834-4838.